Output Energy Maximization Approach for Carrier-Phase Offset Recovery of 8-VSB Signals

Jangwoo Park, Thinh Nguyen, *Member, IEEE*, and Wonzoo Chung, *Senior Member, IEEE*

***Abstract*—This paper presents a blind adaptive carrier-phase offset recovery algorithm based on an output energy maximization approach for eight-level vestigial sideband (8-VSB) signals. Unlike conventional quadrature amplitude modulation signals, the 8-VSB signals in practice have an asymmetric energy balance between the in-phase and quadrature components, which can be used for recovering phase offset, but this has been neglected. We investigate this energy imbalance of the VSB signals and propose a blind adaptive phase offset recovery scheme by maximizing the energy of the in-phase component. Due to the maximum energy property, the proposed algorithm results in superior mean square error performance without undesirable local minima in comparison with the existing phase offset recovery algorithm based on dispersion minimization. We verify the performance of the proposed algorithm with a mathematical analysis and simulation.**

***Index Terms*—Phase offset, vestigial sideband, 8-VSB, adaptive phase offset recovery algorithm.**

I. Introduction

NON-DATA-AIDED, or blind, adaptive algorithms play an important role in the synchronization stage of digital receivers, as synchronization should be done before acquiring training sequences. The carrier phase offset often degrades the system performance of digital receivers, especially for the eight-level vestigial sideband (8-VSB) signals used for Advanced Television System Committee (ATSC) digital television systems in the United States [1]. For 8-VSB signals, the phase offset introduces undesirable leakage of the quadrature component into the in-phase eight-level pulse amplitude modulation (8-PAM) signals. This leakage is modelled as inter-symbol interference (ISI) distortion because the quadrature signal is generated from the in-phase signal via a vestigial sideband (VSB) filter. In this case, the equalizer performance is often degraded in order to mitigate the effect of the VSB filter on the residual quadrature components [2]. Therefore, several blind phase offset recovery algorithms have been studied [3]–[12].

One of the well-studied high-order-statistics blind phase offset recovery schemes is the dispersion minimization (DM) algorithm, which minimizes dispersion of the in-phase component signals [8]. The phase of the DM algorithm is optimized for a one-tap equalizer and tends to produce a channel that is optimized for short equalizers. However, the DM algorithm has undesirable local minima for 8-VSB signals. When the DM algorithm converges on undesirable local minima, the equalizer suffers from significant mean square error (MSE) degradation. Hence, several DM based carrier phase offset recovery algorithms have been proposed to improve the DM algorithm. The decision-directed (DD) approach of the DM algorithm for 8-VSB signals [9] has been proposed to overcome the disadvantages of the high-order-statistics behavior of the DM algorithm. The second-order-based DD approach reduces the computational complexity, but produces undesirable local minima and requires an additional adaptive mechanism to ensure reliable global convergence, which may result in slow convergence. The modified multi-modulus algorithm (MMMA) [12] for 8-VSB signals, a generalized version of [4] and the multi-modulus algorithm (MMA) [5], [6], has been proposed to ensure global convergence without undesirable local minima.

However, none of these methods based on dispersion minimization consider the overall mean-squared-error (MSE) optimality of the receiver when a sufficiently long equalizer is used in the presence of ISI. The DM approach produces the optimal phase for a single-tap equalizer [8], which is not optimal for relatively long equalizers in practice.

In this paper, we propose a low-complexity adaptive blind phase offset recovery algorithm based on second-order statistics, which are free from undesirable local minima and optimized for long equalizers. The strategy is to adjust the phase such that the energy of the in-phase signal is maximized. This approach is similar to the existing output energy maximization (OEM) algorithm, which has been used successfully for timing synchronization [13], but is considered inapplicable for phase offset recovery due to the energy symmetry between the in-phase and quadrature components of most digital signals. For digital VSB signals, however, especially ATSC 8-VSB signals generated by a raised-cosine VSB filter [14], the energy of the quadrature component is smaller

Manuscript received January 21, 2015; revised September 30, 2015 and December 1, 2015; accepted December 27, 2015. This work was supported by the National Research Foundation of Korea under Grant NRF-2013R1A1A2012626.

J. Park and W. Chung are with the Division of Computer and Communications Engineering, Korea University, Seoul 136-713, Korea (e-mail: becks0827@korea.ac.kr; wchung@korea.ac.kr).

T. Nguyen is with the School of Electrical Engineering and Computer Science, Oregon State University, Oregon, OR 97331 USA (e-mail: thinhq@eecs.oregonstate.edu).

Color versions of one or more of the figures in this paper are available online at http://ieeexplore.ieee.org.

Digital Object Identifier 10.1109/TBC.2016.2518623

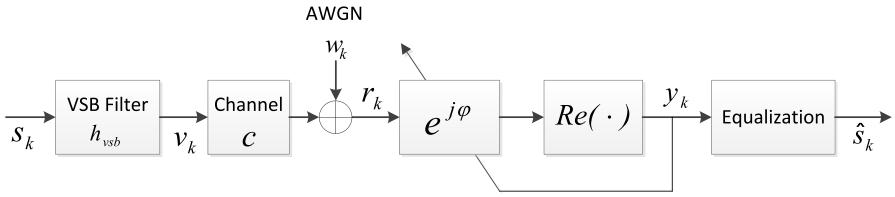

Fig. 1. Discrete-time baseband equivalent 8-VSB system in the presence of phase offset recovery.

than that of the in-phase component due to the loss from the VSB filter. Utilizing this asymmetry, the proposed algorithm successfully recovers the phase offset of 8-VSB signals at low computational cost. Furthermore, the maximized output energy provided by the proposed OEM phase offset recovery algorithm contributes to improving the signal-to-noise ratio (SNR) when the receiver is equipped with a sufficiently long equalizer and consequently helps to achieve near-optimal MSE performance. Briefly, the proposed OEM algorithm is a better fit for a system with a sufficiently long equalizer than the existing algorithms are.

This paper is structured as follows. The energy asymmetry of the in-phase and quadrature components of the 8-VSB signal is investigated in Section II. Section III proposes an adaptive blind phase offset recovery algorithm based on the energy asymmetry, with a cost function analysis. Section IV presents the analysis on tracking ability of the proposed algorithm. The numerical results confirming the performance of the proposed algorithm are shown in Section V, and the conclusion is presented in Section VI.

II. ATSC 8-VSB Signal and System Model

In this section, we introduce the system model of the phase offset recovery algorithm for ATSC 8-VSB signals. Fig. 1 illustrates an overall block diagram of the baseband equivalent VSB system in a discrete time domain. The 8-VSB signal, denoted by $\{v_k\}$, is generated from an independent and identically distributed (i.i.d.) 8-PAM signal at the time k, denoted by $\{s_k\}$, via a VSB filter. The VSB filter used in the ATSC standard is a root-raised cosine filter with the roll-off factor $\beta = 0.1152$. After matched filter processing at the receiver, the resulting VSB filter becomes a raised-cosine filter, as illustrated in Fig. 2. The time domain impulse response of the raised-cosine VSB filter is given as

$$h_{vsb}(t) = e^{j\pi\frac{f_s}{2}t}\frac{\sin(\pi f_s t/2)}{\pi f_s t/2}\frac{\cos\left(\pi\beta\frac{f_s}{2}t\right)}{1-\beta^2 f_s^2 t^2}, \tag{1}$$

where f_s is the symbol rate of the 8-PAM signal ($f_s = 10.76MHz$ in ATSC). Assuming perfect receiver synchronization, the received baseband 8-VSB signal in the absence of multipath channel is then given as

$$r(t) = \sum_{k=-\infty}^{\infty} s_k h_{vsb}(t - kT_s), \tag{2}$$

where T_s denotes the symbol period $T_s = 1/f_s$. In the presence of a multipath channel and white circular complex Gaussian

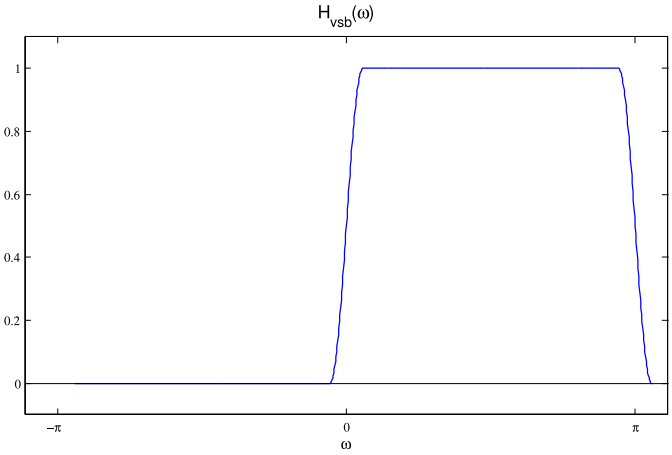

Fig. 2. Frequency response of raised-cosine VSB filter.

noise, denoted by $w(t)$, the baseband received signal can be written as a convolution with a baseband channel model $c(t) = \sum_{i=0}^{N_c-1}\rho_i\delta(t-\tau_i)$,

$$r(t) = \sum_{k=-\infty}^{\infty} s_k \sum_i \rho_i h_{vsb}(t - kT_s - \tau_i) + w(t), \tag{3}$$

where N_c denotes the multipath channel length, ρ_i and τ_i denote the complex multipath attenuation and delay, respectively.

Sampling the $r(t)$ with respect to the sampling period T_s yields baseband received signals in a discrete time domain. Let $\mathbf{r}_k$ denote the infinite length vector consisting of the sampled $r(t)$, *i.e.*, $\mathbf{r}_k = r(kT_s)$. Then, $\mathbf{r}_k$ can be represented by the following discrete time system model:

$$\mathbf{r}_k = \mathbf{c} \star \mathrm{h}_{vsb} \star \mathbf{s} + \mathbf{w}_k, \tag{4}$$

where h_{vsb} denotes the discrete time domain VSB filter given by

$$\mathrm{h}_{vsb}[k] = h_{vsb}(kT_s) = \delta[k] + j\mathrm{h}[k],$$
$$\text{where } \mathrm{h}[k] = \begin{cases} \dfrac{2\cos\left(\frac{\pi}{2}\beta k\right)}{\pi k\left(1-\beta^2k^2\right)} & \text{for odd } k \\ 0 & \text{for even } k \end{cases}, \tag{5}$$

$\mathbf{c} = [c_0, \cdots, c_{N_c-1}]^T$ is the discrete time domain channel model induced from the analog channel $c(t)$, $\mathbf{s} = [\cdots, s_{k-1}, s_k, s_{k+1}, \cdots]^T$ is the transmitted 8-PAM sequence, $\mathbf{w}_k$ denotes the sampled noise at time k, and $\star$ denotes

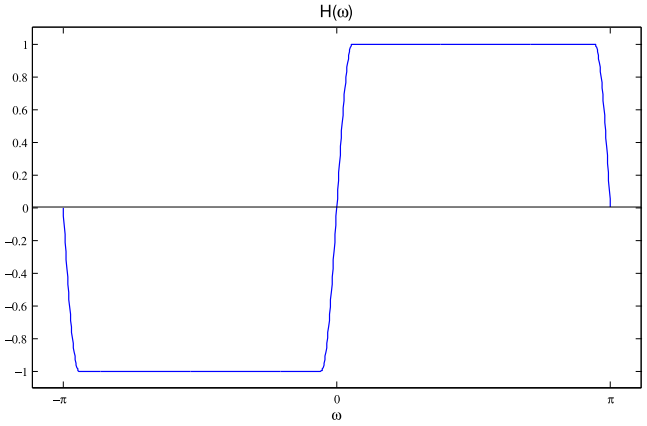

Fig. 3. Frequency response of h[n].

the convolution operation. Note that h[k] has the following frequency response.

$$H(\omega)=\begin{cases}\operatorname{sgn}(\omega), & \frac{\beta}{2}\pi \le |\omega| \le \left(1-\frac{\beta}{2}\right)\pi \\ \cos\left(\frac{\omega}{\beta}-\frac{\pi}{2}\right), & |\omega| < \frac{\beta}{2}\pi \\ \cos\left\{\frac{\omega}{\beta}-\left(\operatorname{sgn}(\omega)\frac{\pi}{\beta}-\frac{\pi}{2}\right)\right\}, & |\omega| > \left(1-\frac{\beta}{2}\right)\pi\end{cases} \tag{6}$$

as illustrated in Fig. 3.

The real component of the matched filter output is processed by an equalizer. Before taking the real component, a phase offset correction is applied

$$\mathrm{y}_k = \operatorname{Re}\left(e^{j\varphi}\mathbf{r}_k\right), \tag{7}$$

The optimal phase φ is the one under which the minimum mean square error (MMSE) equalizer of a given length produces the minimum MSE. However, finding a closed-form expression of such an optimal φ is extremely difficult. Hence, several suboptimal methods for phase offset recovery have been studied [4]–[12]. Of these, the DM algorithm [8] is one of the well-studied blind phase offset recovery schemes, minimizing the following cost function:

$$\varphi_{DM} = \arg\min_{\varphi} E\left[\left\{\operatorname{Re}\left(e^{j\varphi}\mathbf{r}\right)^2-\gamma\right\}^2\right], \tag{8}$$

where γ is a statistical constant called dispersion constant.

The variants of DM algorithms have similar cost functions. The DD phase offset recovery [9] replaces the dispersion constant with 8-PAM decisions $D(\operatorname{Re}(e^{j\varphi}\mathbf{r}))$:

$$\varphi_{DD} = \arg\min_{\varphi} E\left[\left\{\operatorname{Re}\left(e^{j\varphi}\mathbf{r}\right)-D\left(\operatorname{Re}\left(e^{j\varphi}\mathbf{r}\right)\right)\right\}^2\right], \tag{9}$$

The MMA algorithm applied for a blind phase offset recovery scheme minimizes the following cost function [12]:

$$\varphi_{MMA} = \arg\min_{\varphi} E\left[\left\{\operatorname{Re}\left(e^{j\varphi}\mathbf{r}\right)^2-\gamma_R\right\}^2\right] + E\left[\left\{\operatorname{Im}\left(e^{j\varphi}\mathbf{r}\right)^2-\gamma_I\right\}^2\right], \tag{10}$$

where γ_R and γ_I are the dispersion constants for the real and imaginary components, respectively. Because MMA inherits the undesirable local minima of DM, the MMMA [12] has been proposed, which has the following cost function:

$$\varphi_{MMMA} = \arg\min_{\varphi} N\cdot E\left[\left\{\operatorname{Re}\left(e^{j\varphi}\mathbf{r}\right)^2-\gamma_R\right\}^2\right] + M\cdot E\left[\left\{\operatorname{Im}\left(e^{j\varphi}\mathbf{r}\right)^2-\gamma_I\right\}^2\right], \tag{11}$$

where M and N are both real. By choosing appropriate values for M and N, the undesirable local minima of MMMA for 8-VSB can be eliminated. All of the above-mentioned algorithms, *i.e.*, the DM, DD, MMA and MMMA algorithms, basically minimize dispersion, which can be interpreted as optimizing the phase for a single-tap equalizer and may fail to produce optimal performance for a system equipped with a sufficiently long equalizer. Furthermore, depending on the channel, the DM, DD, and MMA algorithms may converge on undesirable local minima, which significantly degrades MSE performance. To overcome these drawbacks of the DM, DD, MMA, and MMMA algorithms for 8-VSB, we propose a blind adaptive algorithm approach for 8-VSB that optimizes the phase for an infinite length equalizer in the following sections.

III. Output Energy Maximization Approach

The goal of the proposed output energy maximization (OEM) phase offset recovery algorithm is to find a phase maximizing the energy of the output y_k, *i.e.*, maximizing the cost function $J(\varphi) = E[\mathrm{y}_k^2]$,

$$\varphi_{OEM} \coloneqq \arg\max_{\varphi} E\left[\operatorname{Re}\left(e^{j\varphi}\mathbf{r}_k\right)^2\right]. \tag{12}$$

The rationale behind this approach is that a sufficiently long equalizer would be able to gather the energy spread over multitaps and yield maximum SNR. An adaptive solution to finding the phase of the OEM algorithm is as follows, according to the general stochastic gradient update rule [15]:

$$\varphi_{k+1} = \varphi_k - \mu\operatorname{Re}\left(e^{j\varphi_k}\mathbf{r}_k\right)\operatorname{Im}\left(e^{j\varphi_k}\mathbf{r}_k\right), \tag{13}$$

where μ is the step size. The phase of the OEM algorithm can be obtained in a closed-form expression by analyzing the cost function $J(\varphi)$. For convenience, let us introduce the following notations:

$$\mathbf{c}_r \coloneqq \operatorname{Re}(\mathbf{c}), \tag{14}$$

$$\mathbf{c}_i \coloneqq \operatorname{Im}(\mathbf{c}), \tag{15}$$

$$\bar{\mathbf{c}}_r \coloneqq \mathrm{h}\star\mathbf{c}_r, \tag{16}$$

$$\bar{\mathbf{c}}_i \coloneqq \mathrm{h}\star\mathbf{c}_i. \tag{17}$$

Then, the equalizer input is written as

$$\begin{aligned}\mathrm{y}_k &= \operatorname{Re}\left(e^{j\varphi}\mathbf{r}_k\right) = \operatorname{Re}\left(e^{j\varphi}\cdot\mathbf{c}\star\mathrm{h}_{vsb}\star\mathbf{s}+e^{j\varphi}\mathbf{w}_k\right)\\ &= \operatorname{Re}((\cos\varphi+j\sin\varphi)(\mathbf{c}_r+j\mathbf{c}_i)\star(\delta[k]+j\mathrm{h})\star\mathbf{s}\\ &\quad+(\cos\varphi+j\sin\varphi)(\operatorname{Re}(\mathbf{w}_k)+j\operatorname{Im}(\mathbf{w}_k)))\\ &= [\cos\varphi(\mathbf{c}_r-\bar{\mathbf{c}}_i)-\sin\varphi(\mathbf{c}_i+\bar{\mathbf{c}}_r)]\star\mathbf{s}\\ &\quad+\cos\varphi\operatorname{Re}(\mathbf{w}_k)-\sin\varphi\operatorname{Im}(\mathbf{w}_k).\end{aligned} \tag{18}$$

Assuming that the signal power is $\sigma_s^2 = E[s_k^2]$, and the noise power is $\sigma_w^2 = E[\mathbf{w}_k^2]$, the cost function of the OEM algorithm $J(\varphi)$ is given by

$$\begin{aligned} J(\varphi) &= E\Big[\mathrm{y}_k^2\Big] = E\Big[\mathrm{Re}\big(e^{j\varphi}\mathbf{r}_k\big)^2\Big] \\ &= E\Big[\big((\cos\varphi(\mathbf{c}_r - \bar{\mathbf{c}}_i) - \sin\varphi(\mathbf{c}_i + \bar{\mathbf{c}}_r)\big) \star \mathbf{s} \\ &\quad + \cos\varphi \mathrm{Re}(\mathbf{w}_k) - \sin\varphi \mathrm{Im}(\mathbf{w}_k)\big)^2\Big] \\ &= E\Big[s_k^2\Big]\cos^2\varphi\|\mathbf{c}_r - \bar{\mathbf{c}}_i\|^2 + E\Big[s_k^2\Big]\sin^2\varphi\|\bar{\mathbf{c}}_r + \mathbf{c}_i\|^2 \\ &\quad - 2E\Big[s_k^2\Big]\sin\varphi\cos\varphi < \mathbf{c}_r - \bar{\mathbf{c}}_i, \bar{\mathbf{c}}_r + \mathbf{c}_i > + \frac{1}{2}E\Big[\mathbf{w}_k^2\Big] \\ &= \sigma_s^2\frac{\|\mathbf{c}_r - \bar{\mathbf{c}}_i\|^2 - \|\bar{\mathbf{c}}_r + \mathbf{c}_i\|^2}{2}\cos(2\varphi) \\ &\quad - \sigma_s^2 < \mathbf{c}_r - \bar{\mathbf{c}}_i, \bar{\mathbf{c}}_r + \mathbf{c}_i > \sin(2\varphi) \\ &\quad + \sigma_s^2\frac{\|\mathbf{c}_r - \bar{\mathbf{c}}_i\|^2 + \|\bar{\mathbf{c}}_r + \mathbf{c}_i\|^2}{2} + \frac{1}{2}\sigma_w^2 \\ &= \begin{cases} A\cos\Big(2\varphi + \tan^{-1}\frac{2<\mathbf{c}_r - \bar{\mathbf{c}}_i, \bar{\mathbf{c}}_r + \mathbf{c}_i>}{B}\Big) \\ \quad + \sigma_s^2\frac{\|\mathbf{c}_r - \bar{\mathbf{c}}_i\|^2 + \|\bar{\mathbf{c}}_r + \mathbf{c}_i\|^2}{2} + \frac{1}{2}\sigma_w^2 & \text{if } B > 0 \\ A\cos\Big(2\varphi - \pi + \tan^{-1}\frac{2<\mathbf{c}_r - \bar{\mathbf{c}}_i, \bar{\mathbf{c}}_r + \mathbf{c}_i>}{B}\Big) \\ \quad + \sigma_s^2\frac{\|\mathbf{c}_r - \bar{\mathbf{c}}_i\|^2 + \|\bar{\mathbf{c}}_r + \mathbf{c}_i\|^2}{2} + \frac{1}{2}\sigma_w^2 & \text{if } B < 0 \end{cases} \end{aligned} \tag{19}$$

where

$$A = \sigma_s^2\sqrt{\frac{B^2}{4} + < \mathbf{c}_r - \bar{\mathbf{c}}_i, \bar{\mathbf{c}}_r + \mathbf{c}_i >^2},$$
$$B = \|\mathbf{c}_r - \bar{\mathbf{c}}_i\|^2 - \|\bar{\mathbf{c}}_r + \mathbf{c}_i\|^2,$$

and $< X, Y >$ denotes the dot product of two vectors, *i.e.*, $< X, Y >= X^H Y$. Hence,

$$\arg\max_{\varphi} J(\varphi) = \begin{cases} -\frac{1}{2}\tan^{-1}\frac{2<\mathbf{c}_r - \bar{\mathbf{c}}_i, \bar{\mathbf{c}}_r + \mathbf{c}_i>}{B} \pm n\pi, & \text{if } B > 0 \\ \frac{\pi}{2} - \frac{1}{2}\tan^{-1}\frac{2<\mathbf{c}_r - \bar{\mathbf{c}}_i, \bar{\mathbf{c}}_r + \mathbf{c}_i>}{B} \pm n\pi, & \text{if } B < 0 \end{cases} \tag{20}$$

where $n = 0, 1, 2, 3, \cdots$.

In the absence of a multipath channel, $\mathbf{c}_i, \bar{\mathbf{c}}_i = 0$ and $\mathbf{c}_r = \delta[k], \bar{\mathbf{c}}_r = \mathrm{h}[k]$, the cost function is given as

$$\begin{aligned} J(\varphi) &= \frac{1 - \|\mathrm{h}\|^2}{2}\sigma_s^2\cos(2\varphi) + \frac{1 + \|\mathrm{h}\|^2}{2}\sigma_s^2 + \frac{1}{2}\sigma_w^2 \\ &= \frac{\beta}{4}\sigma_s^2\cos(2\varphi) + \Big(1 - \frac{\beta}{4}\Big)\sigma_s^2 + \frac{1}{2}\sigma_w^2. \end{aligned} \tag{21}$$

Note that $\|\mathrm{h}\|^2 = 1 - \frac{\beta}{2}$ can be obtained with Parseval's theorem,

$$\begin{aligned} \|\mathrm{h}\|^2 &= \frac{1}{2\pi}\int_{-\pi}^{\pi}|H(\omega)|^2 d\omega = (1 - \beta) \\ &\quad + \frac{2}{\pi}\int_0^{\frac{\beta}{2}\pi}\cos^2\Big(\frac{\omega}{\beta} - \frac{\pi}{2}\Big)d\omega = 1 - \frac{\beta}{2}. \end{aligned} \tag{22}$$

Figure 4 illustrates the cost function of the OEM algorithm in comparison with the DM, DD, MMA, and MMMA schemes. The proposed OEM phase offset recovery algorithm does not show any undesirable local maxima at $\pi/2$, $3\pi/2$, just like MMMA with $(M, N) = (1, -0.444)$, and does have maxima at 0 and π. Note that the OEM algorithm maximizes its cost function, while others minimize their cost functions, and the MMMA always requires a rotation by $\pi/2$ (or $3\pi/2$) to correct the phase offset from its design principle. Figure 5 demonstrates the global convergence of the stochastic algorithm of the proposed OEM algorithm to the desired maxima for the additive white Gaussian noise (AWGN) channel in a severe noise environment for 10dB and 20dB SNR. In the

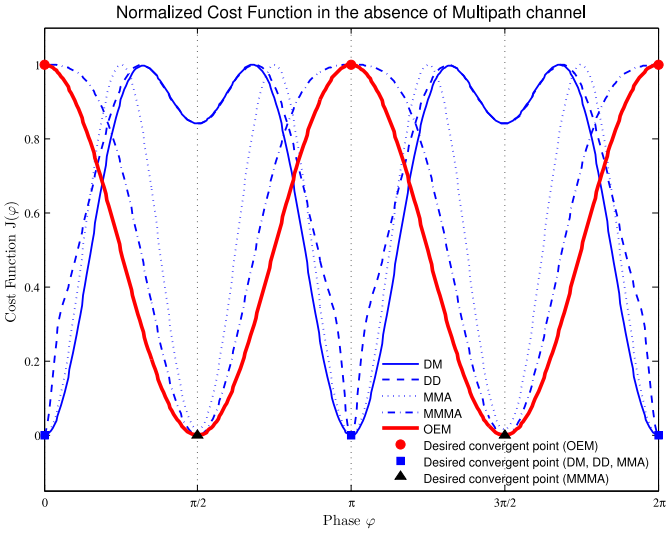

Fig. 4. Cost functions in the absence of multipath channel for 8-VSB using DM, DD, MMA, MMMA with $(M, N) = (1, -0.444)$ and OEM (SNR = 20dB).

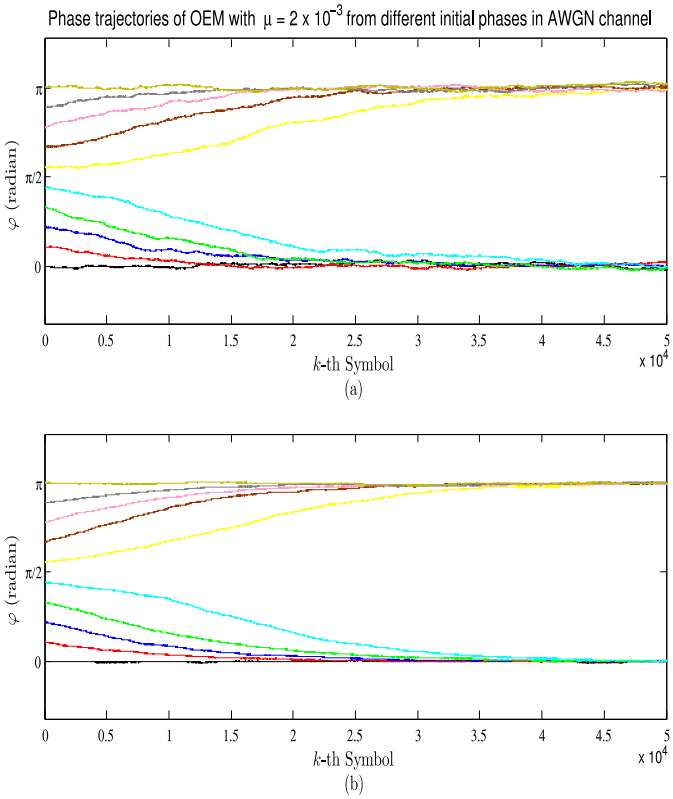

Fig. 5. Phase trajectories of the OEM algorithm with $\mu = 2 \times 10^{-3}$ from different initial phases in AWGN channel ((a) SNR = 10dB, (b) SNR = 20dB).

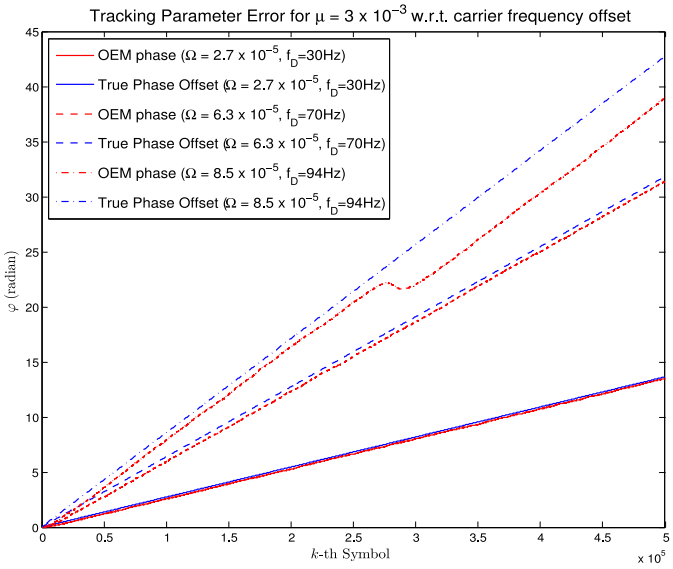

Fig. 6. Tracking Parameter Error for $\mu = 3 \times 10^{-3}$ w.r.t. carrier frequency offset (SNR = 20dB).

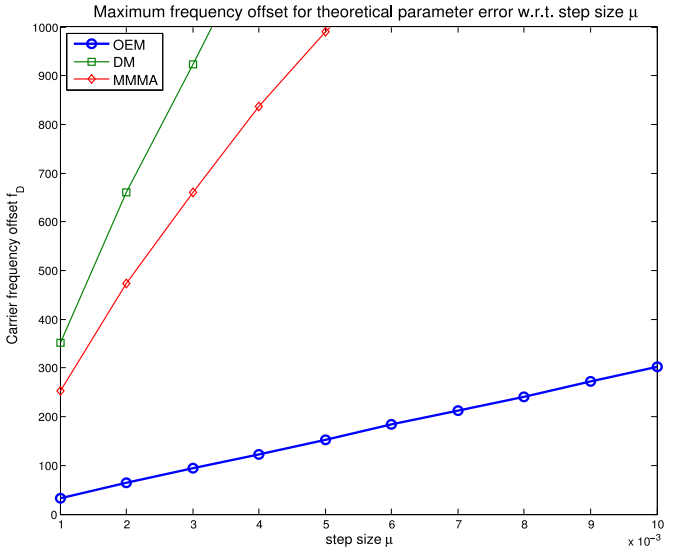

Fig. 7. Maximum frequency offset for theoretical parameter error w.r.t. step size μ (SNR = 20dB).

presence of the ISI channel, the minima of these algorithms become different. The simulation results in Section V show that the proposed OEM algorithm generally results in a better MSE performance for a receiver equipped with a sufficiently long equalizer, compared with existing schemes.

IV. Tracking Ability

The tracking performance is important to carrier phase offset recovery schemes. To investigate the tracking ability of the OEM algorithm, we assumed that the phase offset varies linearly over time at a constant rate Ω. The phase offset at the k-th update is given by $\Phi + k\Omega$ where Φ denotes the initial phase offset. From the update Eq. (13), the phase of the OEM algorithm can be obtained as follows:

$$\varphi_{k+1} = \varphi_k - \mu \mathrm{Re}\Big(e^{j\varphi_k} e^{-j(\Phi+k\Omega)} \mathbf{r}_k\Big) \mathrm{Im}\Big(e^{j\varphi_k} e^{-j(\Phi+k\Omega)} \mathbf{r}_k\Big). \tag{23}$$

Define the parameter error θ_k as

$$\theta_k := \varphi_k - (\Phi + k\Omega). \tag{24}$$

By substituting θ into the Eq. (23), we obtain

$$\theta_{k+1} = \theta_k + \Omega - \mu \mathrm{Re}\big(e^{j\theta_k} \mathbf{r}_k\big) \mathrm{Im}\big(e^{j\theta_k} \mathbf{r}_k\big). \tag{25}$$

Taking the ensemble average of the above system results in the following:

$$E[\theta_{k+1}] = E[\theta_k] + \Omega - \mu \frac{\sigma_s^2}{2} \Big(1 - \|\mathrm{h}\|^2\Big) E[\sin 2\theta_k]. \tag{26}$$

Assume that the parameter error reaches a steady state at the end, *i.e.*, $\lim_{k\to\infty} E[\theta_{k+1}] = \lim_{k\to\infty} E[\theta_k]$, and that Ω is sufficiently small to validate the first-order approximation $\sin 2\theta_k \approx 2\theta_k$ in Eq. (26). Then

$$\theta_\infty := \lim_{k\to\infty} E[\theta_k] \approx \frac{2\Omega}{\mu \sigma_s^2 \beta}. \tag{27}$$

For the ATSC 8-VSB signal, where $\sigma_s^2 = 1$ with $\beta = 0.1152$ and the symbol rate $R_s = 1.1 \times 10^6$, the phase tracking estimation error can be written in terms of the residual frequency offset f_D, which can arise from a phase-locked loop error or a time-varying channel, (*e.g.*, via the Doppler effect).

$$\theta_\infty \approx C \frac{f_D}{\mu}. \tag{28}$$

where $C = 2/(R_s \beta) \approx 1.6 \times 10^{-5}$.

Figure 6 plots the tracking ability of the OEM algorithm for step size $\mu = 3 \times 10^{-3}$ for several residual carrier frequency offsets. The parameter error starts diverging from the value predicted theoretically in Eq. (28) around f_D = 94 Hz. This jump in the tracking error θ comes from the breakdown of the small Ω assumption in Eq. (27). Figure 7 shows the numerically obtained maximum residual carrier frequency offsets that OEM can track within the parameter error predicted in Eq. (28) as a function of the step size μ. The maximum tractable residual carrier frequency increases with the step size. Note that the OEM algorithm has relatively small maximum residual carrier frequency offsets in comparison with the existing DM and MMMA, due to the small difference between the maximum and minimum of the cost function of the OEM algorithm.

V. Simulation Results

In this section, we show the performance of the proposed phase offsetrecovery algorithm via simulation, including that in the presence of a multi-path channel. Let us consider the simple artificial four-tap multipath channel C_1 defined by

$$C_1 = \delta(t) + 0.7e^{j\frac{3}{4}\pi}\delta(t - 6T_s) + 0.6e^{j\frac{3}{2}\pi}\delta(t - 25T_s) + 0.5e^{j\frac{1}{3}\pi}\delta(t - 46T_s).$$

For multipath channel C_1, the phase of the OEM algorithm obtained analytically and numerically is $\varphi_{OEM} = \frac{119}{180}\pi + n\pi$ ($n = \cdots, -1, 0, 1, \cdots$). The phases of DM, DD, MMA,

TABLE I
MULTIPATH PROFILE

Channel	Parameter	Path 1	Path 2	Path 3	Path 4	Path 5	Path 6
ATSC R2.1	Atten. (dB) #4	11	0	11	1	10	9
	Delay (μs)	0	1.8	1.95	3.6	7.5	36.8
	Phase Offset (deg)	125°	0°	80°	45°	0°	90°
ATSC R2.2	Atten. (dB) #2	8	0	3	4	3	12
	Atten. (dB) #3	3	0	1	1	3	9
	Delay (μs)	0	1.8	1.95	3.6	7.5	41.6
	Phase Offset (deg)	125°	0°	80°	45°	0°	90°

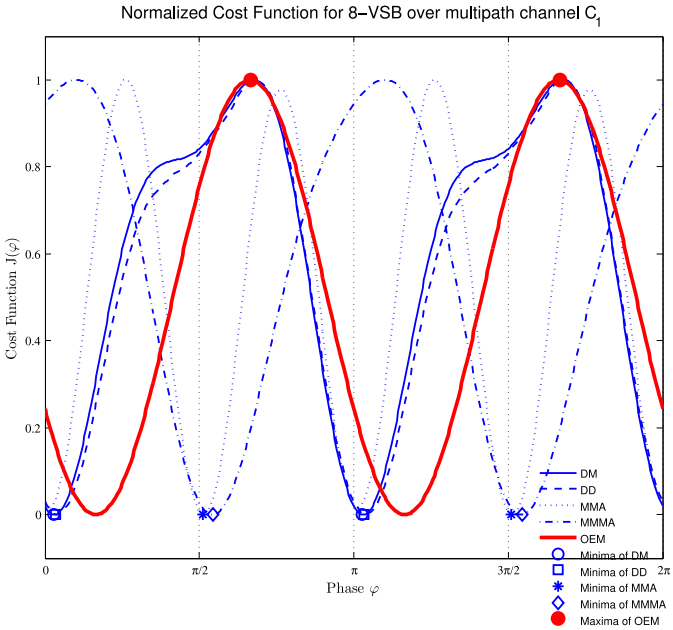

Fig. 8. Normalized cost functions for C_1: DM, DD, MMA, MMMA, and OEM.

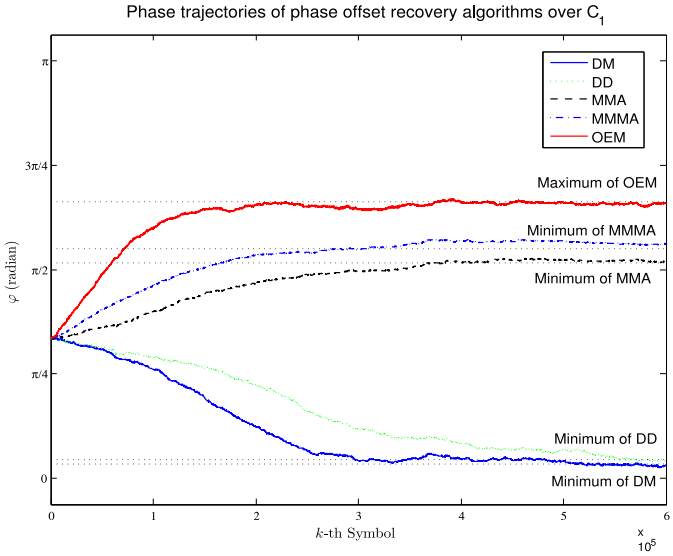

Fig. 9. Phase trajectories of DM, DD, MMA, MMMA, and OEM for C_1. (SNR = 20dB).

and MMMA are all obtained from numerical computation using a stochastic gradient descent algorithm. The phase of the DM algorithm is $\varphi_{DM} = \frac{5}{180}\pi + n\pi$, and the phases of the DD and MMMA (1,-0.444) algorithms are closely located to the phase of the DM algorithm, $\varphi_{DD} = \frac{7}{180}\pi + n\pi$ and $\varphi_{MMMA} = \frac{8}{180}\pi + n\pi$, respectively. The phase of the MMA algorithm is $\varphi_{MMA} = \frac{91}{180}\pi + n\pi$. Figure 8 plots the normalized cost functions of the five algorithms to compare their maxima and minima. Figure 9 plots the phase trajectories of the stochastic gradient descent algorithms converging on each phase solution along the cost functions (note that MMMA requires $\pi/2$ (or $3\pi/2$) shift to implement a stochastic descent gradient). The step sizes μ used for the adaptive algorithms are $\mu_{OEM} = 1 \times 10^{-3}$, $\mu_{DM} = 7 \times 10^{-5}$, $\mu_{DD} = 7 \times 10^{-4}$, $\mu_{MMA} = 3 \times 10^{-5}$, $\mu_{MMMA} = 4 \times 10^{-5}$, respectively.

These different phase values result in different real-valued channels after carrier phase offset recovery of complex channel C_1 and real projection. Depending on the channel, the MMSE equalizer of the channel would result in different MMSE performance, *i.e.*, some channels would be easier to equalize than others. For each channel recovered using each phase solution for C_1, the MSE of the MMSE equalizer of a given length all differ, as compared in Fig. 10. The DM, DD, and MMMA algorithms give a similar MSE, because their phases are located close to each other. The OEM algorithm starts to outperform the existing schemes as the equalizer length increases, and the performance of the MMA is between that of the OEM and the other algorithms. φ_{MMSE} denotes the optimal phase that can produce the minimum MSE performance for a given length of MMSE equalizer. φ_{MMSE} is the best phase one can achieve, and it can be obtained only from an exhaustive numerical search for a given length of equalizer. Figure 10 shows that the performance of the OEM algorithm approaches the MSE of φ_{MMSE} as the equalizer length increases.

We now consider realistic channel models, ATSC R2.1 and R2.2 multipath channels, which are gathered from the field and widely used in ATSC 8-VSB receiver tests [16]. The ATSC R2.1 and R2.2 multipath channel profiles are described in Table I. For these channels, we have found the phases of the OEM, DM, DD, MMA, and MMMA algorithms via corresponding adaptive stochastic descent algorithms under 20dB SNR, as summarized in Table II.

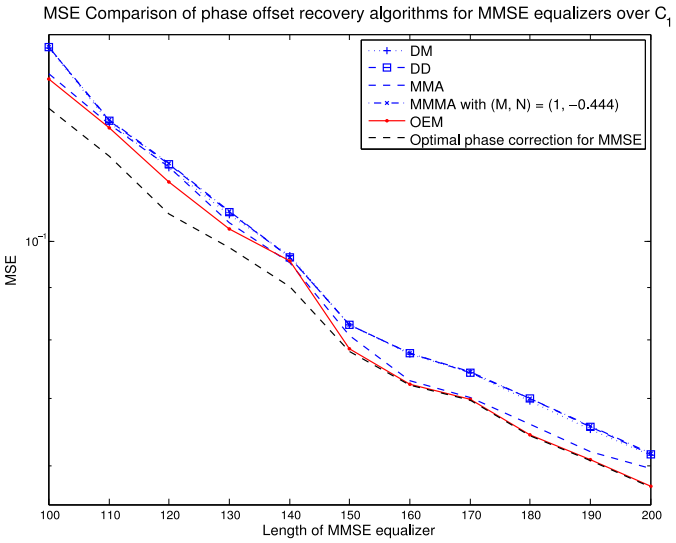

Fig. 10. MSE comparison of phase offset recovery algorithms for MMSE equalizers over C_1 (SNR = 20dB).

TABLE II
PHASE OF VARIOUS PHASE OFFSET RECOVERY ALGORITHMS OVER ATSC MULTIPATH CHANNELS (20dB SNR)

Multipath Channel	φ_{DM}	φ_{DD}	φ_{MMA}	φ_{MMMA}	φ_{OEM}
ATSC R2.1 #4	$\frac{2}{180}\pi$	$\frac{12}{180}\pi$	$\frac{3}{180}\pi$	$\frac{2}{180}\pi$	$\frac{152}{180}\pi$
ATSC R2.2 #2	$\frac{9}{180}\pi$	$\frac{17}{180}\pi$	$\frac{2}{180}\pi$	$\frac{16}{180}\pi$	$\frac{148}{180}\pi$
ATSC R2.2 #3	$\frac{34}{180}\pi$	$\frac{46}{180}\pi$	$\frac{169}{180}\pi$	$\frac{41}{180}\pi$	$\frac{142}{180}\pi$

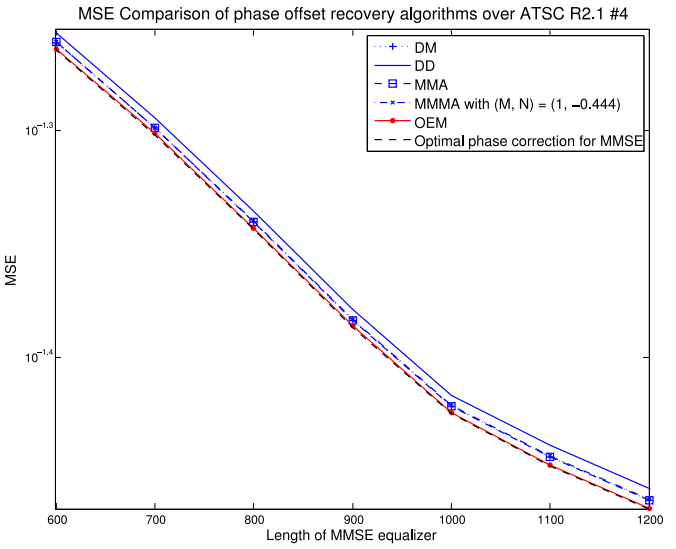

Fig. 11. MSE comparison of phase offset recovery algorithms over ATSC R2.1 #4 multipath channel (SNR = 20dB).

Figure 11–13 show the MSE performance of the DM, DD, MMA, MMMA, and OEM algorithm with respect to the length of MMSE equalizer for each channel. The optimal φ_{MMSE} is found by exhaustive search for each MMSE equalizer length. The simulation results show that the proposed OEM algorithm outperforms existing schemes and approaches near-optimal MSE performance for more than 500 taps. Since equalizers

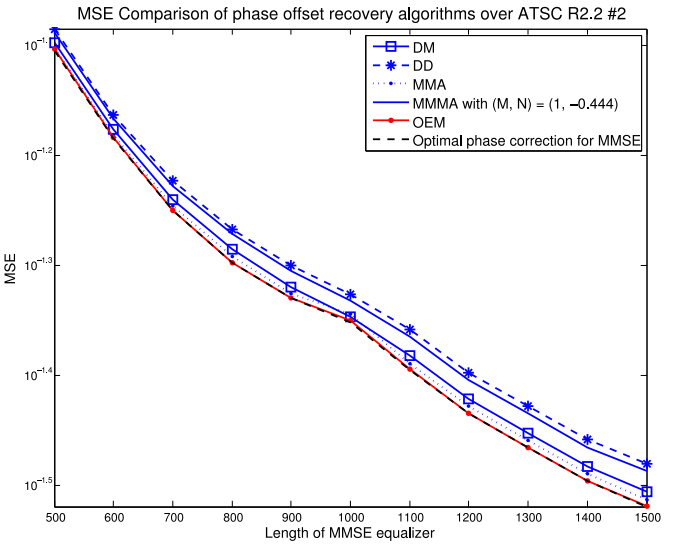

Fig. 12. MSE comparison of phase offset recovery algorithms over ATSC R2.2 #2 multipath channel (SNR = 20dB).

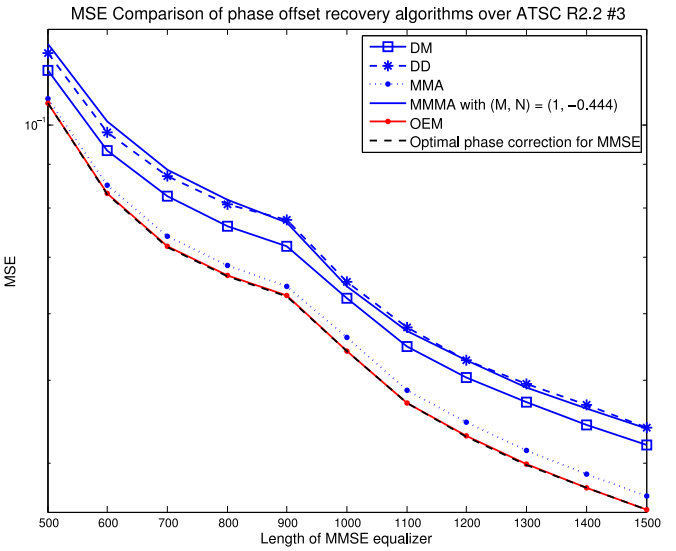

Fig. 13. MSE comparison of phase offset recovery algorithms over ATSC R2.2 #3 multipath channel (SNR = 20dB).

with 500 taps are within the practical range of receiver design, the proposed OEM algorithm is expected to produce near-optimal MSE performance for ATSC multipath channels in practical applications.

VI. CONCLUSION

We proposed a blind adaptive carrier-phase offset recovery algorithm based on an output energy maximization approach for 8-VSB signals. We analyzed the cost function of the OEM algorithm, including the closed-form expression of the phase of the OEM algorithm, and showed unimodality of the proposed algorithm. The phase of OEM algorithm is optimized for a system equipped with a sufficiently long equalizer. The tracking ability of the OEM algorithm is analyzed by studying steady-state parameter error. Simulation results verified the advantage of the OEM algorithm in comparison with the existing algorithms.

REFERENCES

[1] J. G. N. Henderson *et al.*, "ATSC DTV receiver implementation," *Proc. IEEE*, vol. 94, no. 1, pp. 119–147, Jan. 2006.

[2] W. Chung, "A DFE structure using quadrature components of 8-VSB signals," *IEEE Trans. Broadcast.*, vol. 54, no. 3, pp. 394–400, Sep. 2008.

[3] D. N. Godard, "Self-recovering equalization and carrier tracking in two-dimensional data communication systems," *IEEE Trans. Commun.*, vol. COM-28, no. 11, pp. 1867–1875, Nov. 1980.

[4] H. Mathis, "Blind phase synchronization for VSB signals," *IEEE Trans. Broadcast.*, vol. 47, no. 4, pp. 340–347, Dec. 2001.

[5] K. Wesolowski, "Self-recovering adaptive equalization algorithms for digital radio and voiceband data modems," in *Proc. Eur. Conf. Circuit Theory Design*, Paris, France, 1987, pp. 19–24.

[6] K. N. Oh and Y. O. Chin, "Modified constant modulus algorithm: Blind equalization and carrier phase recovery algorithm," in *Proc. IEEE Int. Conf. Commun.*, Seattle, WA, USA, 1995, pp. 498–502.

[7] Y. Wang, E. Serpedin, and P. Ciblat, "Optimal blind nonlinear least-squares carrier phase and frequency offset estimation for general QAM modulations," *IEEE Trans. Wireless Commun.*, vol. 2, no. 5, pp. 1040–1054, Sep. 2003.

[8] W. Chung, W. A. Sethares, and C. R. Johnson, Jr., "Performance analysis of blind adaptive phase offset correction based on dispersion minimization," *IEEE Trans. Signal Process.*, vol. 52, no. 6, pp. 1750–1759, Jun. 2004.

[9] W. Chung, "Decision-directed carrier phase offset recovery scheme for 8-VSB signals," *IEEE Trans. Consum. Electron.*, vol. 53, no. 4, pp. 1288–1292, Nov. 2007.

[10] J. Xia, "A carrier recovery approach for ATSC receivers," *IEEE Trans. Broadcast.*, vol. 54, no. 1, pp. 131–139, Mar. 2008.

[11] W. Liang, J. Chai, Y. Guan, W. Zhang, and D. He, "A robust and adaptive carrier recovery method for Chinese DTTB receiver," *IEEE Trans. Broadcast.*, vol. 54, no. 1, pp. 146–151, Mar. 2008.

[12] J.-T. Yuan and Y.-F. Huang, "Blind carrier phase acquisition and tracking for 8-VSB signals," *IEEE Trans. Commun.*, vol. 58, no. 3, pp. 769–774, Mar. 2010.

[13] D. N. Godard, "Passband timing recovery in an all-digital modem receiver," *IEEE Trans. Commun.*, vol. 26, no. 5, pp. 517–523, May 1978.

[14] *ATSC Digital Television Standard, Part 2—RF/Transmission System Characteristics*, document A/53, Adv. Telev. Syst. Committee, Washington, DC, USA, Dec. 2011.

[15] J. R. Treichler, C. R. Johnson, Jr., and M. G. Larimore, *Theory and Design of Adaptive Filters*. Upper Saddle River, NJ, USA: Prentice Hall, 2001.

[16] *ATSC Recommended Practice: Receiver Performance Guidelines*, document A/74, Adv. Telev. Syst. Committee, Washington, DC, USA, Apr. 2010.

Jangwoo Park, photograph and biography not available at the time of publication.

Thinh Nguyen, photograph and biography not available at the time of publication.

Wonzoo Chung, photograph and biography not available at the time of publication.